

# Study on the Impact of Size and Position of the Shear Field in Determining the Shear Modulus of Glulam Beam Using Photogrammetry Approach

Niaz Gharavi, Hexin Zhang

**Abstract**—The shear modulus of a timber beam can be determined using torsion test or shear field test method. The shear field test method is based on shear distortion measurement of the beam at the zone with the constant transverse load in the standardized four-point bending test. The current code of practice advises using two metallic arms act as an instrument to measure the diagonal displacement of the *constructing square*. The size and the position of the constructing square might influence the shear modulus determination. This study aimed to investigate the size and the position effect of the square in the shear field test method. A binocular stereo vision system has been employed to determine the 3D displacement of a grid of target points. Six glue laminated beams were produced and tested. Analysis of Variance (ANOVA) was performed on the acquired data to evaluate the significance of the size effect and the position effect of the square. The results have shown that the size of the square has a noticeable influence on the value of shear modulus, while, the position of the square within the area with the constant shear force does not affect the measured mean shear modulus.

**Keywords**—Shear field test method, structural-sized test, shear modulus of Glulam beam, photogrammetry approach.

## I. INTRODUCTION

**S**HEAR stresses and shear modulus can sometimes be the limiting factors in designing the timber structures. For instance, relatively deep beams e.g. short span Glulam beams, are subjected to failure in shear. According to BS EN 408 [1], the shear modulus of a structural-size timber beam can be determined using torsion test and shear field test method. Despite the fact that torsional test creates pure shear status in the beam, it does not represent the real-life situation when the beam is in the service [2]. On the other hand, shear field test method is based on four-point bending test which creates similar loading situation as in reality. The latter method is based on the shear distortion measurement of the beam at the zone with the constant transverse loading in the standardized four-point bending test as indicated in BS EN 408 [1].

Current testing code of practice, i.e. [1], advised using two metallic arms (Fig. 1) act as instruments to measure the diagonal distortion of the constructing square (Fig. 3). The diagonals deformation is defined as the shear deformation of the beam. Determination of the shear modulus  $G_{SF}$  of the beam using shear field test method was proposed in details by Brandner et al. [3]. The shear field test method was

included in BS EN 408:2010 [1] following Brandner et al. [3], [4] recommendations for determining the shear modulus of structural timber and glue laminated timber. BS EN 408 has instructed to measure the shear distortion of the beam at the middle of the constant shear span by measuring the changes in diagonals of the marked square (Fig. 3) when subjected to flexural loading. According to BS EN 408, Shear modulus of the beam can be determined using (1).

$$G_{tor,s} = \alpha \frac{h_0(V_{s,2} - V_{s,1})}{bh(w_2 - w_1)} \quad (1)$$

where  $\alpha = \frac{3}{2} - \frac{h_0^2}{4h^2}$ ,  $h_0$  is length of the un-deformed square diagonals (Fig. 3),  $h$  and  $b$  are the cross-sectional depth and width, respectively,  $w_i$  is the mean deformation of both diagonals of the square at both sides of the beam for the given shear load (Fig. 4),  $V_{s,i}$  is the shear load as  $i$  being the load increment.

Although the square size was considered when assigning the shear correction factor ( $\alpha$ ), the impact of the size has not been experimentally investigated. According to Brandner et al. [3] shear correction factor ( $\alpha$ ) can be determined using (2).  $\alpha$  is based on the relationship between shear stress distribution over the whole cross-section of the beam and shear stress distribution over the shear field area (Fig. 2).

$$\alpha = \frac{\tau_{SF}}{\tau_0} + \frac{3}{2} \cdot \left\{ \frac{\tau_{max} - \tau_{SF}}{\tau_0} \right\} \quad (2)$$

In term of the location of the square within the shear constant area, BS EN 408 recommends placing the square in the middle of the span. on the other hand, Brandner et al. [3] placed in the fixed distance of  $d_{SF} = 500mm + L/2$  (Fig. 3). This study aimed to study the impact of the size and position of the constructing square in the shear field test method. Since the recommended apparatus for measuring the shear distortion of the beam is limited to measure only one square at a time, the method is inefficient for this study. Therefore, a binocular stereo vision system was developed to capture the 3D displacement of a grid of target points. This approach is an accurate and non-contact method to extract the 3D coordination of targeted object using two cameras. Six glue laminated beams were produced and tested according to the guideline given in BS EN 408. Analysis of Variance (ANOVA) was performed on the acquired data to evaluate the impact of size and position of the square in the determination of shear modulus of the beam.

N. Gharavi is with School of Engineering and the Built Environment at Edinburgh Napier University, Edinburgh EH10 5DT UK (phone: +44(0) 131 455 2249; e-mail: n.gharavi@napier.ac.uk).

H. Zhang is with School of Engineering and the Built Environment at Edinburgh Napier University, Edinburgh, EH10 5DT UK (phone: +44(0) 131 455 2482; e-mail: j.zhang@napier.ac.uk).

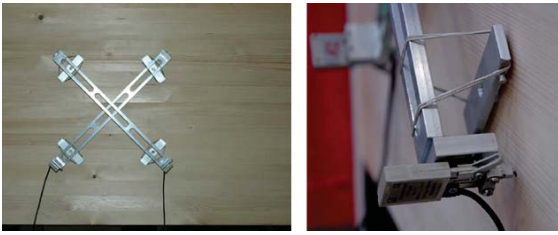


Fig. 1 Metallic arms to measure the diagonal distortion [1]

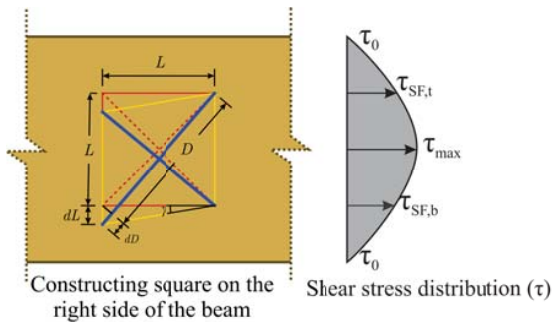


Fig. 2 Shear Field and shear stress distribution

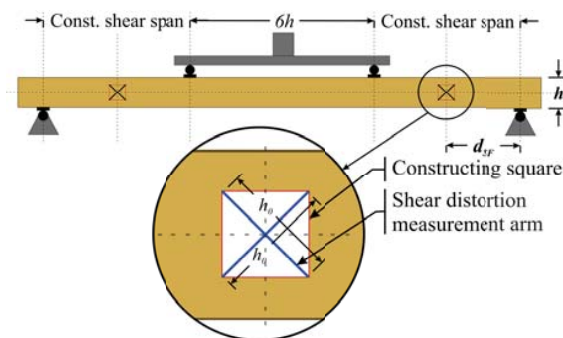


Fig. 3 Shear field's constructing square before deformation

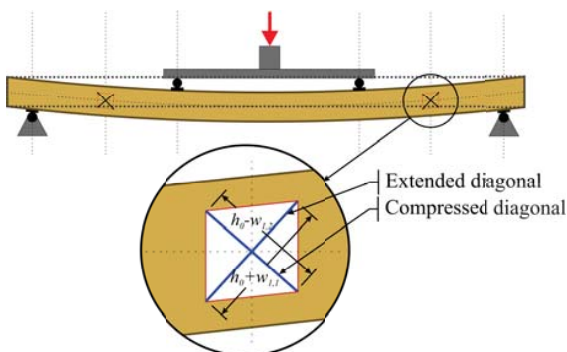


Fig. 4 Shear field's constructing square after deformation

## II. MATERIALS AND METHOD

### A. Materials

Six laminated beams were produced using five timber and laminated bamboo lumber (LBL) laminae. Three of the laminated beams were constructed as hybrid beams with three layers of timber and two layers of LBL. While the other three laminated beams were constructed with five layers of timber. The beams were then tested in four-point bending test according to specifications given in BS EN 408 [1]. The flexural properties and shear modulus of the beam can be determined with the aforementioned bending test. The beams were subjected to loading parallel to their glue lines. Each specimen was constructed with the dimensions of  $142.5 \times 190 \times 3000$  mm, and then reduced to  $142.5 \times 178 \times 3000$  mm to trim the excessive glues and flatten the surfaces. In term of components, the commercially available laminated bamboo worktop made of Moso bamboo with a nominal dimension of  $40 \times 620 \times 3000$  mm were used. As for the timber, Norway Spruce timbers with strength class of C24 according to BS EN 338 [5] and the nominal dimensions of  $45 \times 195 \times 3600$  mm were used. The timbers were then cut and planed to the required dimensions of  $28.5 \times 190 \times 3000$  mm. For the optimum bonding strength between laminae, the planing were conducted within 24 hours of glueing. Phenol-Resorcinol Formaldehyde Resin (PRF) (Cascosinol Phenol Resorcinol Adhesive 1711 with Hardener 2520) produced by AKZO NOBEL, with minimum glue spread of  $425 \text{ g/m}^2$  single-sided were applied. All the components were conditioned for a period of four weeks before and after lamination.

### B. Stereo Vision System

The conventional method of measuring the displacement in the structural tests is through mechanical gauges such as LVDTs, rotation measuring gauges, etc.. These devices possess several limitations; they are limited to measure only one point and the physical interaction between measuring gauges and the specimen is often unavoidable. While, lasers and optical measurement systems can be deployed for higher accuracy, but these devices are expensive. Because of these limitations conventional methods could not be used in this research. Stereo Vision System is a triangulation-based approach, which allows us to determine the three-dimensional coordinates of any targeted point in the world and/or camera coordinate systems at any desired time [6]. Depending on the processing tasks, stereo vision can sometimes be expensive in term of computational requirements [7]. Due to the low data processing load in this experiment, the system was set up and executed fairly inexpensive. Binocular vision system is similar to the method used by human and most of the animal's eyes for depth perception. The system works by taking two images of a scene of interest simultaneously from different positions and angles. Binocular Stereo Vision is a well-known method of acquiring the 3D information of a target and have been used in many applications in variety of industries, e.g. robotic, industrial quality inspection, etc. The employed system has described in details in the author's previous research work [8].

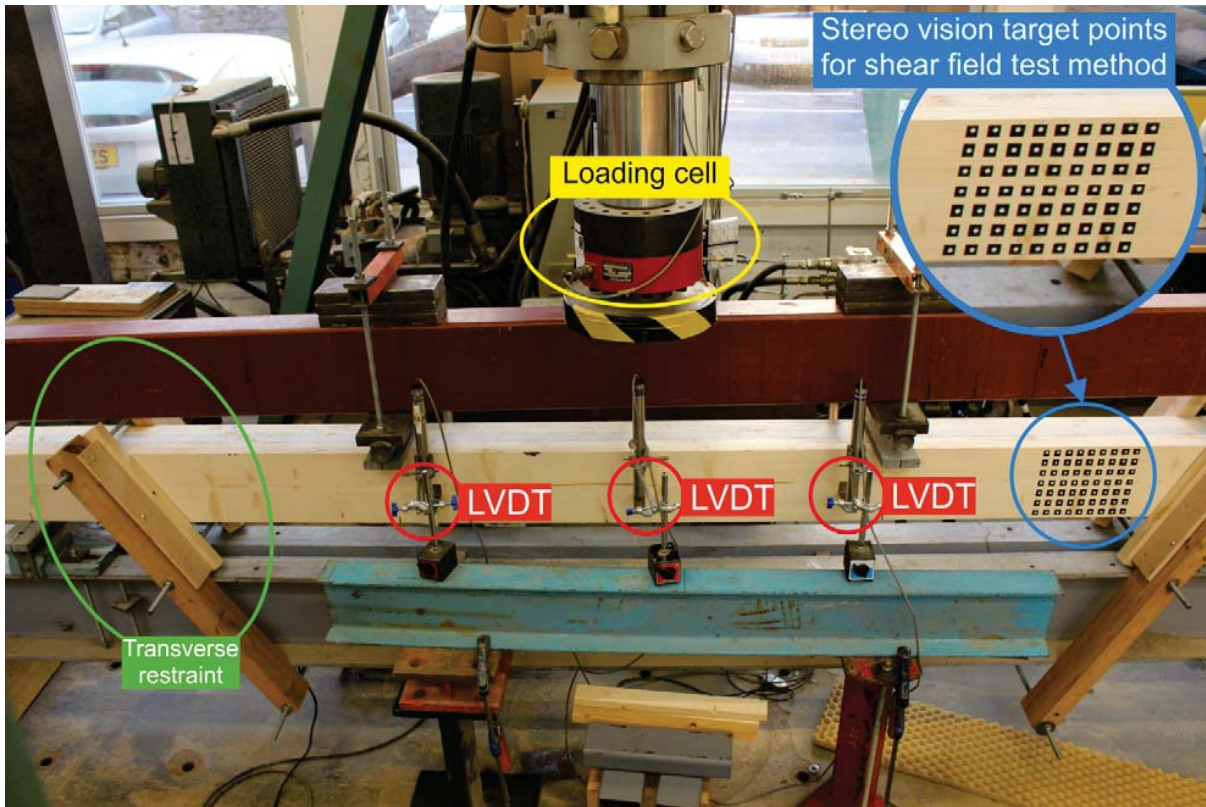


Fig. 5 Four-point bending test image

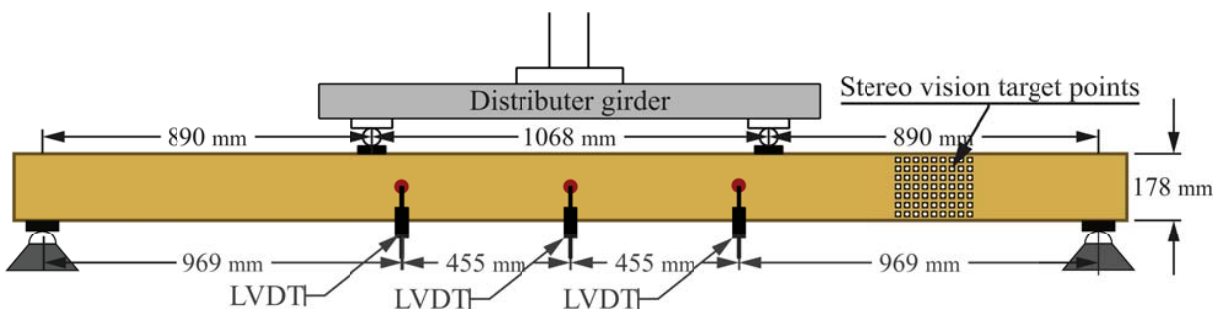


Fig. 6 Four-point bending test setup configuration

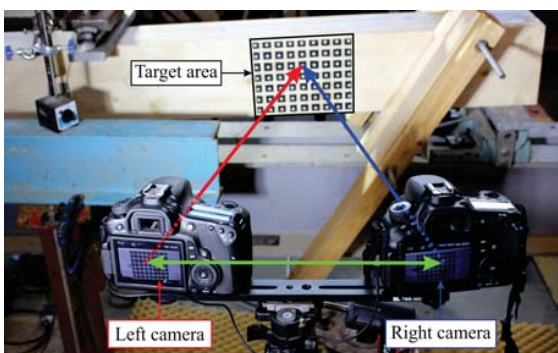
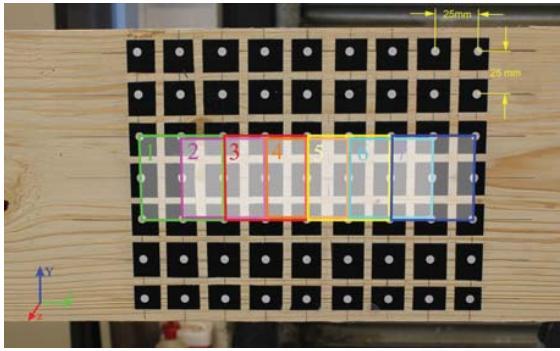
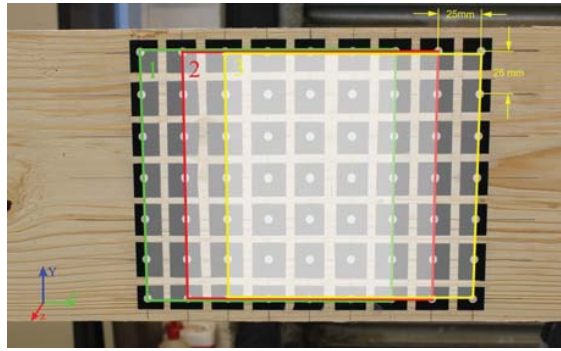
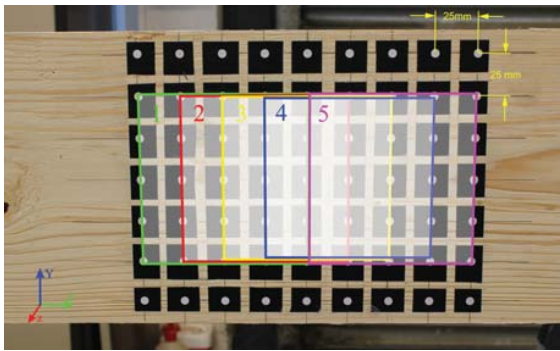
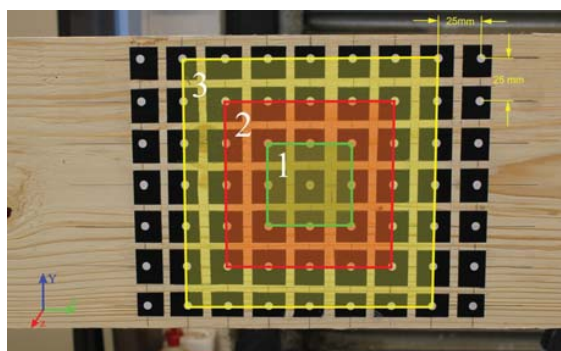


Fig. 7 Employed stereo vision system

### C. Shear Field Test Method

The shear field test was conducted following the specifications given in BS EN 408 [1]. The test is based on the measuring the shear deformation of the beam in the constant shear force area in the four-point bending test (Fig. 6). Each specimen was supported vertically and transversely. The vertical supports were spanned 16 times the cross-sectional depth ( $h$ ), while the lateral restraints were provided to prevent any transverse displacement (Fig. 5). The loading was applied at the constant rate of 0.10 mm/sec. The vertical displacement of the beam at the shear-free span was recorded using six LVDTs at both sides of the beam, while the shear deformation was captured by stereo vision system using two *Canon EOS 70D* cameras on one side and two *Canon EOS 550D* cameras on the other. All the cameras were equipped with 50 mm



Fig. 8 Constructing squares in the case *One*Fig. 10 Constructing squares in the case *Three*Fig. 9 Constructing squares in the case *Two*Fig. 11 Constructing squares in the case *Four*

Canon EF f/1.8 II fix focal lenses (Fig. 7). The cameras captured the images every 5kN load increment simultaneously till the fracture happened. The captured images were processed using MvTec HALCON to extract the 3D coordinates of each target point in world coordinate system. Comparing every step with the initial coordinate of any target point reveals the displacement of the point in three dimensions.

The target points were mapped on the side beams in a grid-like layout (Fig. 8). Each target point can be considered as a corner of a square. Therefore, several squares with different size and positions can be drawn using these target points (Figs. 8-11). Using each constructing square, the shear modulus of the beam can be determined following (1). Four cases were considered to be analysed based on the square size and dimension (Figs. 8-11). Cases *One*, *Two* and *Three* evaluate the impact of the square position using small, medium and large size squares, respectively. Case *Four* evaluates the impact of the square size when the squares placed at the centre of the constant shear span. The squares in each model are symmetric to the neutral axis, this is due to the fact that the shear field test method is based on symmetric shear stress distribution over the cross-section of the beam (Fig. 2) [3].

### III. RESULTS

The overall flexural properties, i.e Modulus of Elasticity (MOE) and Modulus of Rupture (MOR), and the shear modulus of the tested specimens are given in Table I. The calculated shear modulus of the beams is based on the medium-size square which symmetrically placed at the

centre of the constant shear span (Square #2 in Fig. 11). The calculated mean shear modulus of the BTHB is 1355 MPa, showing 14% higher in comparison to timber control glue-laminated beams (1187 MPa).

Analysis of Variance (ANOVA) has been carried out on the impact of the size and the position of the square in the determination of the shear modulus of the beam. The impact of the square position in the constant shear span area has been evaluated using ANOVA for the cases *One*, *Two* and *Three*. The study was based on the position of three type of squares with different dimensions as can be seen in Figs. 8-10. Each square was spaced 25 mm from adjusting squares. The calculated shear modulus of the beams for each cases can be found in Tables II-IV. The ANOVA analysis has indicated that the position of the square is not an important factor in the determination of the shear modulus of a beam. This, clearly, confirms with the constant shear deformation of a beam within the constant shear force area in the Four-Point bending test. Although, in the areas close to the loading or support the deformation changes due to Saint Venant's end effect.

On the other hand, the impact of the size of the constructing square on the variation of the shear modulus of the beam was analysed in case *Four*. As it can be seen from Fig. 11, three squares with different dimensions were selected and based on the distortion of each square corresponding shear modulus has determined. The shear modulus of each beam against the square sizes, i.e. Small, Medium and Large, are given in Table V. The null hypothesis for the impact of square size was set to; "The size of the square will have no

TABLE I  
FOUR POINT BENDING AND SHEAR FIELD TESTS RESULTS

Specimen	MOE (GPa)	MOR (MPa)	G (MPa)
4P-G1	12.65	37.58	1276.21
4P-G2	14.82	36.21	1155.63
4P-G3	14.22	45.36	1130.31
4P-H1	12.94	45.48	1478.64
4P-H2	11.14	43.97	1258.22
4P-H3	14.84	48.67	1328.96

MOE: Modulus of Elasticity; MOR: Modulus of Rupture; G: Shear Modulus  
4P: 4-Point bending; H: Hybrid beam; G: Glulam control beams;  $i$ : {1,2,3}

TABLE II  
MEASURED SHEAR MODULUS BASED ON SMALL SQUARES (FIG. 8)

Sq. No.	4P-G1	4P-G2	4P-G3	4P-H1	4P-H2	4P-H3
1	1299.1	1054.2	1214.2	1225.6	1282.9	1117.2
2	1257.2	1012	1096.5	1137.0	1533.6	1187.2
3	1269.3	1132.5	1163.9	1306.3	1259.2	1262.1
4	1239.1	1311.5	1082.7	1394.4	1224.8	1226.8
5	1249.3	1284.1	1057.7	1555.6	1171.2	1177.9
6	1269.1	1201.4	1092.3	1423.1	1113.6	1282.9
7	1351	1148.2	1173.2	1287.4	1059.5	1172.4
Mean	<b>1282.5</b>	<b>1163.4</b>	<b>1125.8</b>	<b>1332.8</b>	<b>1235.0</b>	<b>1203.8</b>
CoV[%]	<b>2.98</b>	<b>9.55</b>	<b>5.13</b>	<b>10.35</b>	<b>12.45</b>	<b>4.75</b>

impact on the variation of the shear modulus of the tested beam". The ANOVA factor,  $F(2, 15) = 3.84$ , for the size impact rejects the null hypothesis. This implies that the size of the square will have an impact on the determination of the shear modulus. Based on the results of this experiments, measured shear modulus of the beam increased with the square size in five out of six tested samples. The higher determined shear modulus in large squares may be due to heterogeneous characteristics of wood and non-uniform deformation near the edges of the timber. More research needs to be undertaken on the significance of the impact of the square size in the determination of the shear modulus for different cross-sections and species.

#### IV. CONCLUSIONS AND RECOMMENDATIONS

The size and position of the *constructing square* in the shear field test method were examined using ANOVA analysis. The following conclusions can be drawn based on the results of this experiment:

TABLE V  
MEASURED SHEAR MODULUS OF THE BEAM BASED ON SQUARE SIZE (FIG. 11)

Sq. No.	4P-G1	4P-G2	4P-G3	4P-H1	4P-H2	4P-H3
Small square	1239.2	1311.5	1082.7	1394.4	1224.8	1226.827
Medium square	1276.2	1155.6	1130.3	1478.6	1258.2	1328.96
Large square	1384.0	1222.9	1375.7	1595.3	1412.9	1775
CoV[%]	<b>5.79</b>	<b>6.36</b>	<b>13.15</b>	<b>6.77</b>	<b>7.73</b>	<b>20.20</b>

- The results of this study indicated that the size of the square has an impact on the mean shear modulus of a timber beam. It is recommended that the measuring square with the edge length of one-half of the cross-sectional depth is an appropriate setup. Further research is required in order to draw a solid conclusion regarding the significance of this impact.
- the position of the square within the constant shear force area is not an affecting factor in the mean shear modulus. Yet, the minimum distance of the measuring square from the loading or supporting points is to be investigated.
- Stereo vision systems are highly beneficial in the mechanical tests. These systems allow us to measure the 3D displacement of several target points simultaneously without physical contact.

#### ACKNOWLEDGEMENTS

The authors would like to gratefully acknowledge the financial support provided by Lawrence Ho Research Fund and Peter KK Lee PhD Studentships. The help and assistance of Roshan Dhonju in the production and testing stages are greatly appreciated.

#### REFERENCES

- [1] BSI, *BS EN 408:2010+A1:2012: Timber structures - Structural Timber and Glued Laminated Timber - Determination of Some Physical and Mechanical Properties*. London, UK: The British Standards Institution, 2010.
- [2] D. S. Riyanto and R. Gupta, "A Comparison of Test Methods for Evaluating Shear Strength of Structural Lumber," *Forest Products Journal*, vol. 48, no. 2, pp. 83–90, 1998.
- [3] R. Brandner, B. Freytag, and G. Schickhofer, "Determination of shear modulus by means of standardized four-point bending tests," in *CIB W18*, no. August, St. Andrews, Canada, 2008, pp. 41–21–1.
- [4] R. Brandner, E. Gehri, T. Bogensperger, and G. Schickhofer, "Determination of modulus of shear and elasticity of glued laminated timber and related examinations," in *CIB W18*, Bled, Slovenia, 2007, pp. 40–12–2.
- [5] BSI, *BS EN 338:2016: BSI, Structural Timber Strength Classes*. London, UK: The British Standards Institution, 2016.
- [6] C. Wohler, *3D computer vision: efficient methods and applications*, 2nd ed. London, UK: Springer, 2013.
- [7] A. Valsaraj, A. Barik, P. Vishak, and K. Midhun, "Stereo Vision System Implemented on FPGA," *Procedia Technology*, vol. 24, pp. 1105–1112, 2016.
- [8] N. Gharavi, H. Zhang, Y. Xie, and T. He, "End effect on determining shear modulus of timber beams in torsion tests," *Construction and Building Materials*, vol. 164, pp. 442–450, 2018.

TABLE III  
MEASURED SHEAR MODULUS BASED ON MEDIUM SQUARES (FIG. 9)

Sq. No.	4P-G1	4P-G2	4P-G3	4P-H1	4P-H2	4P-H3
1	1266	1116.7	1148.4	1359.5	1261.2	1136.9
2	1258.2	1122.9	1154	1465.7	1296.2	1340.6
3	1276.2	1155.6	1130.3	1478.6	1258.2	1329
4	1297.8	1162	1135.9	1421.4	1313.7	1365
5	1377	1277.2	1193	1400.6	1176.3	1287.8
Mean	<b>1321.5</b>	<b>1197.0</b>	<b>1170.7</b>	<b>1380.1</b>	<b>1218.7</b>	<b>1212.4</b>
CoV[%]	<b>3.72</b>	<b>5.55</b>	<b>2.14</b>	<b>3.41</b>	<b>4.20</b>	<b>7.04</b>

TABLE IV  
MEASURED SHEAR MODULUS BASED ON LARGE SQUARES (FIG. 10)

Sq. No.	4P-G1	4P-G2	4P-G3	4P-H1	4P-H2	4P-H3
1	1412.6	1216.8	1344.5	1604.7	1418	1279.2
2	1384	1222.9	1375.7	1595.3	1412.9	1775.1
3	1415.3	1235.8	1409.5	1583.7	1536.2	1670.2
Mean	<b>1413.9</b>	<b>1226.3</b>	<b>1377.0</b>	<b>1594.2</b>	<b>1477.1</b>	<b>1474.7</b>
CoV[%]	<b>1.23</b>	<b>0.79</b>	<b>2.36</b>	<b>0.66</b>	<b>4.79</b>	<b>16.59</b>